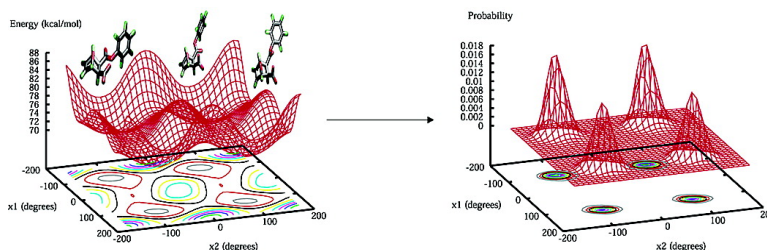


Role of Entropy in Increased Rates of Intramolecular Reactions

Anthony A. Armstrong, and L. Mario Amzel

J. Am. Chem. Soc., **2003**, 125 (47), 14596-14602 • DOI: 10.1021/ja0344359 • Publication Date (Web): 04 November 2003

Downloaded from <http://pubs.acs.org> on March 30, 2009



More About This Article

Additional resources and features associated with this article are available within the HTML version:

- Supporting Information
- Links to the 1 articles that cite this article, as of the time of this article download
- Access to high resolution figures
- Links to articles and content related to this article
- Copyright permission to reproduce figures and/or text from this article

[View the Full Text HTML](#)



Role of Entropy in Increased Rates of Intramolecular Reactions

Anthony A. Armstrong and L. Mario Amzel*

Contribution from the Department of Biophysics and Biophysical Chemistry, Johns Hopkins University School of Medicine, 725 North Wolfe Street, Baltimore, Maryland 21205-2185

Received January 31, 2003; E-mail: mario@neruda.med.jhmi.edu

Abstract: The rates of intramolecular condensation of a series of monoesters of dicarboxylic acids have been shown to be highly dependent on the nature of the intervening groups. To understand the origin of this effect, we estimated $\Delta S_{\text{NAC,S}}$, the entropy difference between the ensemble of accessible ground state conformers and a single ground state conformer having transition-state-like geometry. $\Delta S_{\text{NAC,S}}$ differs from the activation entropy for the reaction by $\Delta S_{\text{TS,NAC}}$, the difference in vibrational entropy between the selected ground state conformer and the transition state. The estimated values of $\Delta S_{\text{NAC,S}}$ correlate well ($R^2 = 0.96$ and 0.73 using dielectric constant values of 80 and 1 , respectively) with experimentally determined reaction rate constants. Normal-mode analysis performed on minimized ground state conformations of each molecule suggests that the change in vibrational entropy makes only a small contribution to the total activation entropy. These results indicate that the conformational entropy difference between the transition and the ground states contributes significantly to the free energy of activation.

1. Introduction

Small molecules undergoing intramolecular cyclization reactions frequently have been used as models for understanding the nature of preorganizational effects and their relative contributions to the enhanced rates observed in enzymatic reactions.^{1–6} (Some authors argue, however, that electrostatic preorganization of the enzyme active site itself represents the largest contribution to the catalytic power of the enzyme.⁷) Even in such comparatively simple systems, much controversy remains.⁸ In 1960, Bruice and Pandit experimentally determined the rates of cyclic anhydride formation for a series of substituted *p*-bromophenyl esters of glutaric, succinic, and 3,6-endo- Δ^4 -tetrahydrophthalic acids.⁹ Reaction rates were observed to increase by a factor of up to ~ 250 per rotatable bond either frozen or eliminated between reactive groups in the series. Rate enhancements, although of a lesser magnitude, were also observed when bond rotation was restricted by placing bulky geminal substituents at the α and β positions. These rate enhancements were attributed to “the resultant decrease in unprofitable rotamer distribution.”⁹ Furthering this work, Bruice and Bradbury showed experimentally that, in an expanded series of mono- and disubstituted monophenyl esters of glutarate, the activation enthalpy remained constant suggesting that the

observed effect on rate was entropic in origin.¹⁰ In a recent computational study, however, Lightstone and Bruice¹ suggested that the trend observed in the reaction rates shows little or no correlation with entropic contributions and could be explained by purely enthalpic considerations. In view of this discrepancy, it is important to reinvestigate this problem.

Thermal integration over conformational space yields the partition function from which the configurational entropy may be calculated, but this procedure remains computationally prohibitive for all but the simplest of small molecules. The configurational integral may, however, be approximated by considering only a subset of “important” internal coordinates,¹¹ traditionally chosen as the dihedral angles of the molecule. This is particularly useful in estimating changes in conformational entropy. In the approach used here, adiabatic mapping, dihedrals of interest were constrained at each point along a grid scan search and the structure was minimized before energies were calculated. Adiabatic mapping was employed by Lee et al.¹² to calculate the change in side chain entropy in binding and folding processes. This procedure was also used by D’Aquino et al.¹³ to calculate the change in entropy that takes place when small flexible organic molecules are restricted to a single rotameric well. In this paper, we report the results of a similar procedure using a grid scan conformational search coupled with constrained minimization to estimate the relative entropies of activation for cyclic anhydride formation in the Bruice and Pandit series of monoesters of dicarboxylic acids. The calcula-

- (1) Lightstone, F. C.; Bruice, T. C. *J. Am. Chem. Soc.* **1996**, *118*, 8, 2595.
- (2) Bruice, T. C.; Lightstone, F. C. *Acc. Chem. Res.* **1999**, *32*, 2, 127.
- (3) Jencks, W. P. *Catalysis in Chemistry and Enzymology*; McGraw-Hill: New York, 1969.
- (4) Schultz, P. G. *Acc. Chem. Res.* **1989**, *22*, 2, 287.
- (5) Bruice, T. C.; Brown, A.; Harris, D. O. *Proc. Natl. Acad. Sci. U.S.A.* **1971**, *68*, 658.
- (6) Page, M. I.; Jencks, W. P. *Proc. Natl. Acad. Sci. U.S.A.* **1971**, *68*, 1678.
- (7) Villa, J.; Strajbl, M.; Glennon, T. M.; Sham, Y. Y.; Chu, Z. T.; Warshel, A. *Proc. Natl. Acad. Sci. U.S.A.* **2000**, *97*, 11899.
- (8) Menger, F. M. *Acc. Chem. Res.* **1985**, *18*, 8, 128.
- (9) Bruice, T. C.; Pandit, U.K. *J. Am. Chem. Soc.* **1960**, *82*, 2, 5858.

- (10) Bruice, T. C.; Bradbury, W. C. *J. Am. Chem. Soc.* **1968**, *90*, 3808.
- (11) Karplus, M.; Kushick, J. N. *Macromolecules* **1981**, *14*, 325.
- (12) Lee, K. H.; Xie, D.; Freire, E.; Amzel, L. M. *Proteins: Struct., Funct., Genet.* **1994**, *20*, 68.
- (13) D’Aquino, J. A.; Freire, E.; Amzel, L. M. *Proteins: Struct., Funct., Genet.* **2000**, *Suppl 4*, 93.

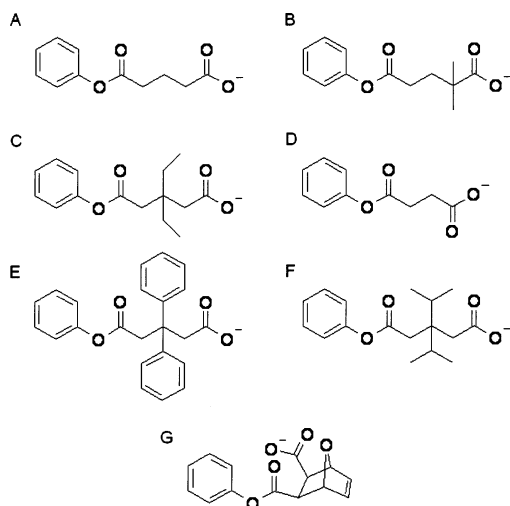


Figure 1. Structures of small molecules considered in this study: the monophenyl esters of (A) glutarate (GLUT), (B) α -gem-dimethylglutarate (α GDMG), (C) β -gem-diethylglutarate (β GDEG), (D) succinate (SUCC), (E) β -gem-diphenylglutarate (β GDGP), (F) β -gem-diisopropylglutarate (β GDIG), and (G) 3,6-endo- Δ^4 -tetrahydrophthalate (36ETHP)

tions show that there is a significant correlation between the estimated entropy differences and the experimentally determined relative rate constants of cyclization.

2. Methods

Energy Calculations. Residue topology files (RTFs) for the molecules shown in Figure 1 were generated using the Quanta (Accelrys, Inc.; San Diego, Ca) suite of modeling software. Subsequent generation of conformations and energy calculations were done within the CHARMM¹⁴ software package. The initial coordinates of each molecule were subjected to 1000 steps of conjugate gradient energy minimization. Conformations for each structure were generated by a grid scan search about all dihedral angles between the two carboxyl moieties. Step sizes of 10° and 20° were used about terminal and internal dihedrals, respectively. At each increment, a constraint was placed on all dihedrals undergoing grid scan rotation, and the coordinates were subjected to 1000 steps of conjugate gradient minimization. Energies were calculated without constraints. The mapping procedure was carried out twice using dielectric constant values of 1 and 80. Although the CHARMM potential function and parameter set have been optimized for calculations on biomacromolecules, its ability to accurately reproduce experimentally determined rotational barriers for small organic molecules has been demonstrated elsewhere.¹⁵

Entropy Calculations. The probability of a given conformation can be calculated as

$$p_i = \frac{e^{-E_i/kT}}{\sum_i e^{-E_i/kT}} \quad (1a)$$

where the sum is carried out over the points of the energy landscape. Calculated probabilities were used to compute ground state entropic terms according to the equation

$$S = -k \sum_i p_i \ln p_i \quad (1b)$$

For each molecule, we then estimated $\Delta S_{\text{NAC},S}$, the difference between the entropy of a single ground state conformer having a geometry resembling that of the transition state and that of all conformers in the energy landscape. $\Delta S_{\text{NAC},S}$ differs from ΔS^\ddagger , the activation entropy, by the difference $\Delta S_{\text{TS},\text{NAC}}$ between the entropy of the chosen conformer and that of the transition state. That is,

$$\Delta S^\ddagger = \Delta S_{\text{NAC},S} + \Delta S_{\text{TS},\text{NAC}} \quad (2)$$

If one assumes that $\Delta S_{\text{TS},\text{NAC}}$ is the same for all the studied compounds, all estimated values of $\Delta S_{\text{NAC},S}$ differ from the corresponding ΔS^\ddagger by the same constant. Lightstone and Bruice¹ have defined a near attack conformation (NAC) as a conformation in which reacting orbitals are aligned and in close proximity but have not yet begun to overlap. The geometric criteria defined for the NACs of the present series of compounds are that the attacking oxygen be within 3.2 Å of the carbonyl carbon and fall within a cone of 30° centered 15° off the normal to the plane of the carbonyl.¹ The energetics of NACs per se have no effect on the kinetics of the reaction: NACs are only useful as surrogates of the transition state that have the advantage that they can be analyzed using standard parameters. The conformer we chose in computing the difference $\Delta S_{\text{NAC},S}$ and refer to as the NAC conformer was the conformer containing the largest number of conformations fulfilling these criteria. Two methods of calculating $\Delta S_{\text{NAC},S}$ were employed. The sum in eq 1b was computed with the index running either over all generated conformations (method 1) or over binned conformations or conformers (method 2). The entropic contributions to $\Delta S_{\text{NAC},S}$ differ between the two methods but share the same tendencies.

Method 1. The change in entropy was computed according to the equation

$$\Delta S_{\text{NAC},S} = -kN \left\{ \sum_i^{\text{Dihed.}} \left[\sum_j p_{ij} \ln p_{ij} \right] - \sum_k^{\text{AllConf.}} p_k \ln p_k \right\} \quad (3)$$

The rightmost summation corresponds to the ground state and is calculated using all grid points on the computed potential energy surface; the subscript k references individual conformations. The double sum on the left-hand side of the subtraction treats the transition-state-like conformer (chosen as the potential energy well containing the largest number of conformations satisfying the geometric criteria for a NAC). The subscript j references points along a slice through the well minimum, and the subscript i denotes the dimension of the slice (i.e., the dihedrals allowed to vary). Points referenced by subscript j were obtained as follows. For each backbone dihedral i , a slice corresponding to a rotation about that dihedral was fit with a quadratic equation about the conformer minimum using thermal weighting. The decision of what range of data points to fit was made somewhat arbitrarily upon visual inspection of each slice; in light of this, weighting of the data was necessary to accurately reproduce the shape of the well. The fitted curve was sampled over 120° at intervals corresponding to those used in calculating the complete energy landscape (see below). Conformational probabilities were calculated along each slice by eq 1, and the entropy difference $\Delta S_{\text{NAC},S}$ was then computed using eq 3.

In mapping the energy landscape, sampling was not uniform about internal and terminal rotatable bonds. To compare differences in entropy between structures differing in the number of rotatable bonds, it was therefore necessary to normalize the calculated values with respect to a common sampling interval. This normalization is given by

$$\Delta S_{(N_0)} = \Delta S_{(N_1)} + R \ln \left(\frac{N_0}{N_1} \right) \quad (4)$$

N_1 and N_0 are the number of sampled conformational states and the number of states to which the entropy term is being normalized,

(14) Brooks, B. R.; Bruccoleri, R. E.; Olafson, B. D.; States, D. J.; Swaminathan, S.; Karplus, M. *J. Comput. Chem.* **1983**, *4*, 187.

(15) Smith, J. C.; Karplus M. *J. Am. Chem. Soc.* **1992**, *114*, 801.

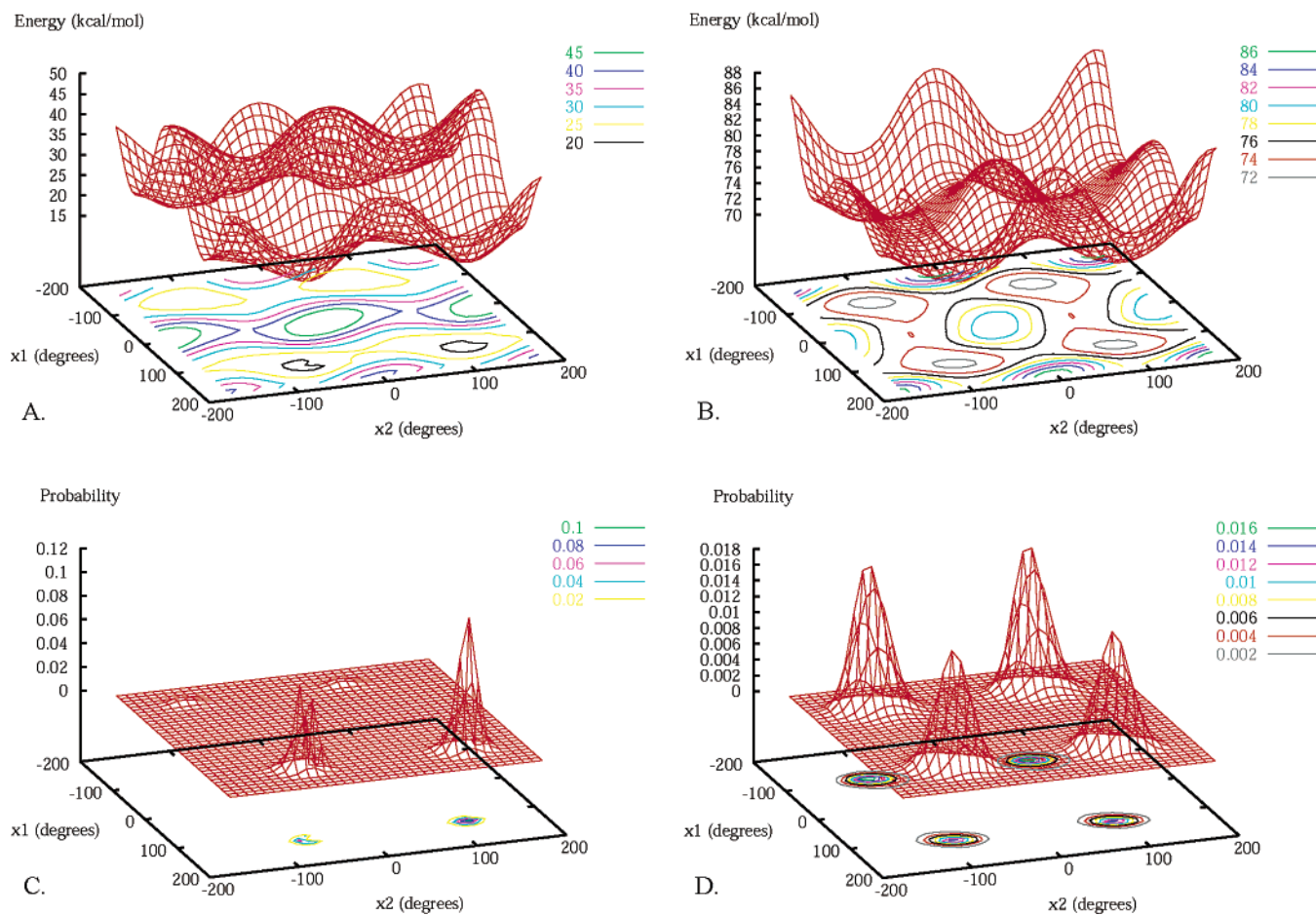


Figure 2. Energy (A,B) and probability (C,D) profiles for structure 36ETHP at constant dielectric values of 1 (A,C) and 80 (B,D). χ_1 and χ_2 refer to the torsional rotations about the bonds between the ring and the carbonyl and carboxylate carbons, respectively.

Table 1. Agreement between Ground State Entropic Terms Calculated Using “Fine” Sampling (A) and “Coarse” Sampling (B) Followed by Normalization to the Fine Sampling Interval for Structures SUCC and 36ETHP (Dielectric Value of 80)^a

	(A) no. of points	entropic term	(B) no. of points	normalized entropic term
SUCC	46 656	17.147	23 328	17.127
36ETHP	129 600	18.083	1296	18.082

^a Sampling intervals are as indicated in the text. Entropic terms are symmetry corrected (i.e., $-R \ln 2$ for symmetry in the last rotatable bond) and *do not* represent a difference as computed in eq 3. Entropic terms are given in entropy units (eu).

respectively. $\Delta S_{(N_1)}$ and $\Delta S_{(N_0)}$ are the non-normalized and normalized entropic terms, respectively. The derivation of this equation, given by D’Aquino et al.,¹³ assumes only that the energy landscape is slowly varying. We normalized all ground state entropic terms calculated by method 1 to a sampling interval of 10°.

Method 2. This method is based on the procedure used by Creamer and Rose¹⁶ to estimate entropies of amino acid side chains. However, instead of using Monte Carlo sampling we used a grid scan search of the accessible conformations as described. For this calculation the grid was subdivided into rotameric bins (conformers). Rotation about a bond between two sp^3 hybridized atoms was divided into three bins: $(-120^\circ, 0^\circ)$, $(0^\circ, 120^\circ)$, $(120^\circ, -120^\circ)$. Rotation about a bond between an sp^3 hybridized atom and an sp^2 hybridized atom was divided into six bins: $(-150^\circ, -90^\circ)$, $(-90^\circ, -30^\circ)$, $(-30^\circ, 30^\circ)$, $(30^\circ, 90^\circ)$, $(90^\circ, -$

$150^\circ)$, $(150^\circ, -150^\circ)$. Thus, a total of 324 rotameric bins were constructed for the esters of glutaric acid, 108 for the ester of succinic acid, and 36 for the ester of phthalic acid. Ranges were selected to bracket the observed minima in the energy profiles for the various structures. The probability of a given conformer was then calculated as the sum of the probabilities for the individual conformations comprising that conformer. An NAC conformer (or alternatively the transition state itself) was modeled as those conformations comprising a single energy well, and $\Delta S_{NAC,S}$ (or the conformational component of the activation entropy $\Delta S_{Conform.}^\ddagger$) was estimated as the entropy difference between the ground state comprising all conformers and a single conformer:

$$\Delta S_{Conform.}^\ddagger = \Delta S_{NAC,S} = -k \sum_i^{All} p_i \ln p_i \quad (5)$$

The sum is now over conformers rather than individual grid points, and the entropy of the single conformer (NAC conformer or transition state) makes no contribution ($p = 1.0$)

Estimation of Vibrational Entropy by Normal-Mode Analysis. Each conformation generated during the grid scan search was fully minimized without constraints. Redundant conformations were discarded, and normal modes were calculated for each unique conformation using the VIBRAN set of commands in CHARMM. The EXPLORE feature was used to step along each mode computing the energy at regular intervals, and a quadratic fit of the energies with Gaussian and Boltzmann weighting options was used to adjust calculated frequencies.

(16) Creamer, T. P.; Rose, G. D. *Proc. Natl. Acad. Sci. U.S.A.* **1992**, *89*, 5937.

Table 2. Experimental Relative Rate Constants^a (k_{rel}) for the Cyclization of the *p*-Bromophenyl Monoester Equivalents of the Compounds Shown in Figure 1 and the Symmetry Corrected Entropy Differences ($\Delta S_{\text{NAC},s}$) Calculated Using Constant Dielectric Values of 1 and 80^a

	no. of points	k_{rel}	$\ln k_{\text{rel}}$	EPS 1			EPS 80			
				no. of energy minima	ΔS (eu) ($-T\Delta S$ (kcal/mol))		no. of energy minima	ΔS (eu) ($-T\Delta S$ (kcal/mol))		vib
					method 1	method 2		method 1	method 2	
GLUT	419 904	1.0E+03	6.9	56	-9.048 (2.698)	-4.505 (1.343)	60	-15.355 (4.578)	-9.180 (2.737)	-2.160
α GDMG	419 904	3.6E+03	8.2	72	-10.292 (3.069)	-5.090 (1.518)	70	-13.813 (4.118)	-8.210 (2.448)	-2.234
β GDEG	419 904	1.8E+05	12.1	114	-8.582 (2.559)	-4.523 (1.349)	56	-10.395 (3.099)	-6.526 (1.946)	-1.858
SUCC	23 328	2.3E+05	12.3	14	-6.125 (1.826)	-3.494 (1.042)	18	-11.090 (3.306)	-7.274 (2.169)	-1.117
β GDPG	419 904	2.7E+05	12.5	112	-8.727 (2.602)	-4.659 (1.389)	91	-9.725 (2.900)	-6.060 (1.807)	-1.709
β GDIG	419 904	1.3E+06	14.1	100	-6.555 (1.954)	-2.597 (0.774)	114	-10.545 (3.144)	-6.559 (1.956)	-2.487
36ETHP	1296	8.0E+07	18.2	4	-3.163 (0.943)	-0.793 (0.236)	6	-5.294 (1.578)	-3.413 (1.018)	-0.352

^a Values of $-T\Delta S$ ($T = 298.15$ K) are provided in parentheses below each entropy estimate. Vibrational entropy differences were calculated using a constant dielectric value of 80. Also shown for each molecule is the number of conformations generated by the grid scan search procedure.

Adjusted frequencies were used to calculate the vibrational entropy associated with each conformational well according to

$$\frac{S}{R} = \sum_{i=1}^n \frac{\theta_i/T}{e^{\theta_i/T} - 1} - \ln(1 - e^{-\theta_i/T}) \quad (6)$$

where $\theta_i = (h\nu_i/k)$, T is temperature, h is Planck's constant, k is Boltzmann's constant, ν_i are the mode frequencies, and the subscript i references the normal mode ($n = 3N - 6$; N = number of atoms). An upper bound to the magnitude of the changes in vibrational entropy upon interconverting between conformers was estimated by subtracting the lowest from the highest of these vibrational entropies.

3. Results and Discussion

Molecular interpretation of the data of Bruice and Pandit⁹ requires establishing a correlation between the structures of the compounds and the free energies of activation (ΔG^\ddagger) of the anhydride formation reaction. We use $\ln k_{\text{rel}}$ as the experimental value directly related to ΔG^\ddagger . In the context of transition state theory, only two structures are relevant to this free-energy change: the substrate(s) and the transition state. Although it is known that the transition state for these reactions involves a tetrahedral intermediate, neither the structures nor the force constants are known well enough to calculate changes of energy and entropy. In this work, following the suggestion of Lightstone and Bruice,¹ we use NACs, ground state conformations closest to the transition state, to estimate relative values of the activation entropy. The entropic differences we calculate, however, are conceptually different from those calculated by Lightstone and Bruice.¹ Lightstone and Bruice calculated two different entropic quantities, one a vibrational entropy difference between two individual ground state conformers and the other a difference between all fully minimized ground state conformations and all fully minimized NACs. We instead calculate $\Delta S_{\text{NAC},s}$, the difference between *all* accessible ground state conformers and a *single* ground state conformer resembling the transition state. (This is not to say each molecule has only one conformer comprising NACs.) $\Delta S_{\text{NAC},s}$ differs from the activation entropy by a quantity $\Delta S_{\text{TS},\text{NAC}}$. Within a family of compounds such as the one studied here, the energetics of forming the transition state from a NAC ($\Delta S_{\text{TS},\text{NAC}}$) should be very similar for all the

compounds: the same tetrahedral intermediate with similar partial charges is generated in all cases, and by definition the NAC is a ground state geometry closely resembling that of the transition state. The value $\Delta S_{\text{TS},\text{NAC}}$ is not a conformational entropy difference; it represents the configurational entropy difference between two conformers, a single NAC conformer and the transition state, rather than between two ensembles involving multiple conformers. Thus, it can be expected that the differences in entropy between each transition state and a NAC conformer are constant or at least proportional to $\Delta S_{\text{NAC},s}$. In either case, if ΔS^\ddagger is linearly correlated with the logarithm of the rate constant k_{rel} , $\Delta S_{\text{NAC},s}$ will show the same correlation. Based on these considerations, we calculated $\Delta S_{\text{NAC},s}$ for each of the compounds to determine if there is a correlation between ΔS^\ddagger and $\ln k_{\text{rel}}$.

All information pertaining to entropy differences between conformational states of a molecule is contained in its energy landscape.¹¹ Well shape reflects the vibrational structure of a particular conformer, and relative shapes and depths combine to determine the conformer distribution. To estimate $\Delta S_{\text{NAC},s}$ in a series of monophenyl esters of dicarboxylic acids (Figure 1), we determined the adiabatic potential energy surface for each molecule using a grid scan conformational search coupled with constrained minimization. The adiabatic approximation allows small clashes at each grid point to be partially relieved through relaxation of bonds, angles, and peripheral torsions. Thus, the energy landscape computed in this manner contains the points with the lowest energies in the landscape (i.e., those that contribute most to the entropy) for all values of the backbone dihedrals. To speed computations, sampling intervals of 10° and 20° were chosen for terminal and internal dihedral angles, respectively, and the computed entropic terms were then normalized by eq 4 to a sampling interval of 10° for all dihedral angles. (We use "entropic term" rather than "entropy" to indicate that these are not absolute entropies and are sampling interval dependent.) To demonstrate that the chosen sampling intervals are not too large with respect to the rate of change of the potential energy surfaces, we also calculated ground state entropic terms by eq 1 for 36ETHP using a sampling interval of 1° about both its dihedral angles and for SUCC using a

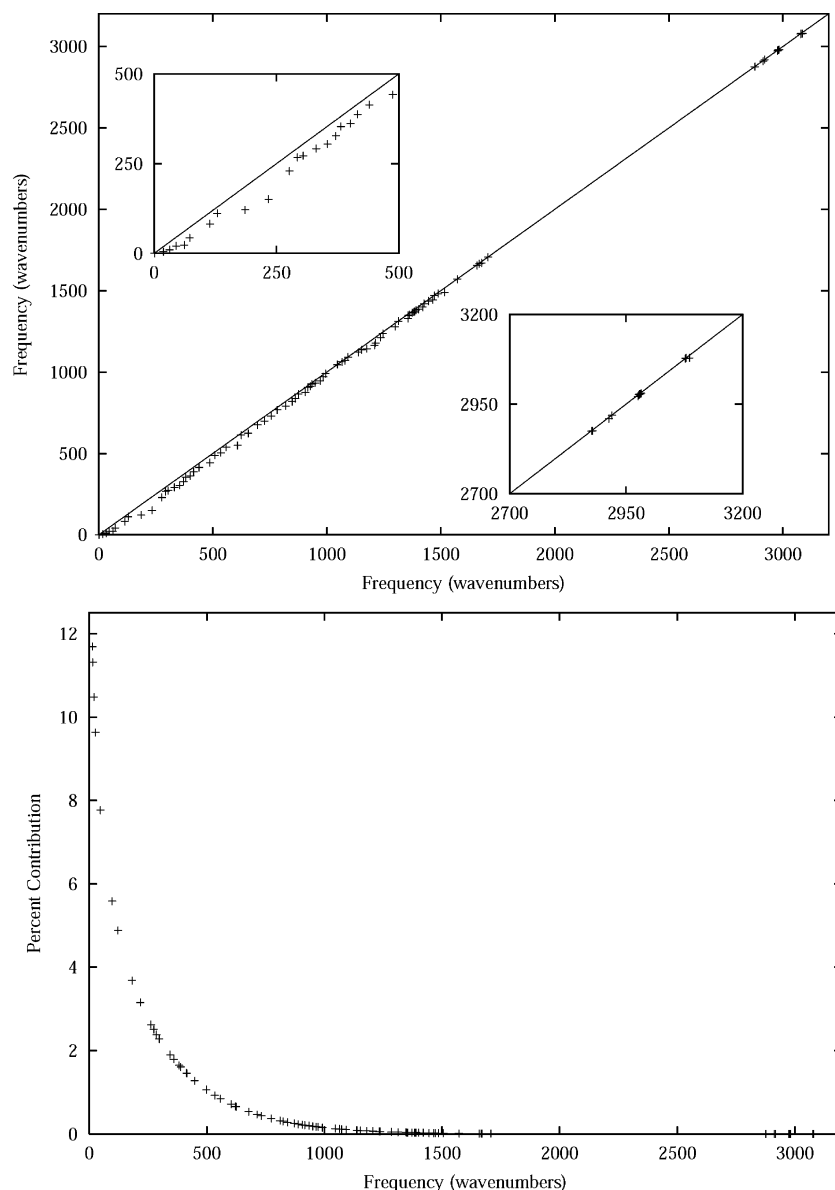


Figure 3. Comparison of normal-mode frequencies of different conformers of α GDMG. The normal modes for each unique fully minimized conformation of structure α GDMG were ordered by increasing frequency. Plotted are the lowest versus the highest frequency for each mode among all conformations (top) and the percent contribution to the vibrational entropy versus frequency for each mode of a randomly selected conformation (bottom). Results are representative for all seven molecules considered.

sampling interval of 10° for all three of its rotatable bonds. These values were compared to the values calculated with the standard sampling (10° and 20° about terminal and internal rotatable bonds, respectively) and subsequently normalized to the same number of points. The results are shown in Table 1.

Figure 2 shows the calculated energy and probability surfaces for 3,6-endoxo- Δ^4 -tetrahydrophthalate (36ETHP) computed with two different values of the dielectric constant, 1 and 80. These values were chosen to bracket the dielectric constant of the solution used in obtaining the experimental data (50% dioxane/water; see below). The bicyclic framework of 36ETHP effectively sets the value of the central dihedral between the two reactive groups; thus for this compound, the grid scan search involved only two rotatable bonds. The surfaces show that the exaggerated electrostatic interactions that result from the use of a gas phase dielectric have a notable effect on the calculated probabilities: only two conformers appear to be significantly populated when this dielectric is used, whereas four equally

populated conformers are observed when interaction energies are calculated using a dielectric of 80. In Table 2, we report the entropy differences $\Delta S_{\text{NAC,S}}$ calculated for each molecule according to eqs 3 (method 1) and 5 (method 2) and give cited values for the experimentally determined relative rate constants.

The vibrational component of the entropy of individual conformers was evaluated in the calculations of Lee et al.¹² by approximating the shape of the potential energy well as that of a simple harmonic oscillator, extracting the force constant, and subsequently determining the entropy of the oscillator using eq 6. We used a similar approach here to estimate the differences in vibrational entropy among ground state conformers. For each molecule, vibrational entropies were calculated according to eq 6 using frequencies obtained by normal-mode analysis performed at all minima in the calculated energy landscapes. Minimum energy conformations were identified by fully minimizing without constraints all conformations generated in the grid scan search and discarding redundant conformations.

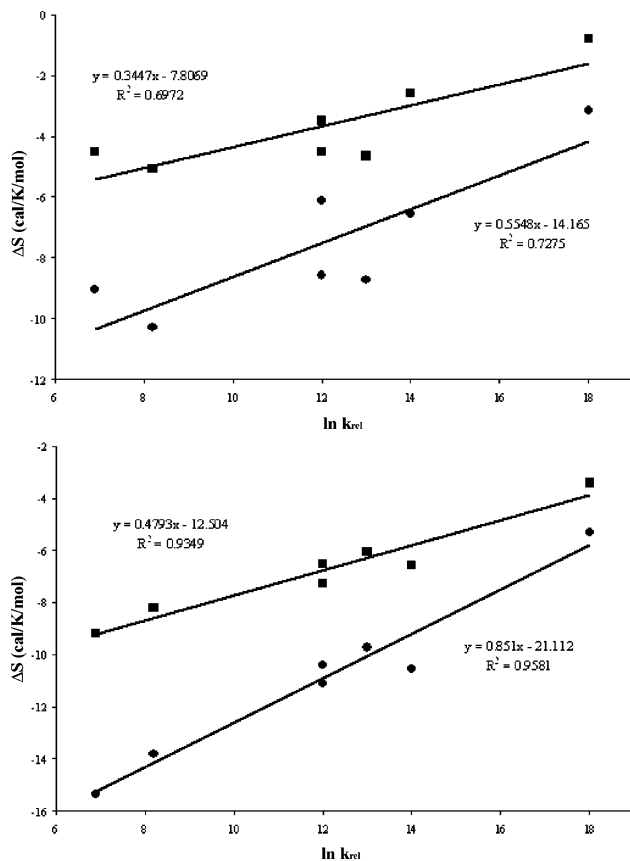


Figure 4. Plots showing calculated values of $\Delta S_{NAC,S}$ versus experimentally determined relative rate constants. Calculations were performed using dielectric constants of 1 (top) and 80 (bottom). Circles and squares indicate values calculated by methods 1 and 2, respectively.

(The minimized conformations were in close agreement with the conformations identified at the minima of the calculated energy landscapes.) An improved estimate of the vibrational frequencies was obtained by determining a quadratic fit to an energy profile generated by stepping along each of the resultant normal modes. Boltzmann and Gaussian weighting factors ensured that any high energy points corresponding to clashes or strained geometries did not contribute significantly to the fit. A comparison of the frequencies among minimized conformations of the same molecule (Figure 3A) shows that the largest differences in frequency occur for the low frequency modes. This result is important, as lower frequency motions contribute more to the vibrational entropies (Figure 3B) calculated by eq 6. The highest and lowest vibrational entropies for each molecule were used as an estimate of the upper limit of the vibrational entropy change that *can* occur between any single ground state conformer and an NAC conformer. Values for all molecules were small, being less than 2.5 e.u. Furthermore, this value is an overestimate due to errors introduced by computational problems such as incomplete minimization. Not surprisingly, the vibrational entropy difference was smallest for 36ETHP (0.35 eu) which has only four symmetry related minima.

In Figure 4, the entropy differences calculated by methods 1 and 2 are plotted against the logarithm of the experimentally determined rate constants for anhydride formation by the *p*-bromophenyl esters corresponding to each of the molecules depicted in Figure 1 (rate constants are relative to that for the reaction between acetate and *p*-bromophenylacetate). The

observed correlation is in agreement with the experimental results of Bruce and Bradbury.¹⁰ It is clear that using a gas phase dielectric results in a poorer correlation, likely because it overemphasizes electrostatic contributions (Figure 2) masking other terms in the CHARMM potential function. Experimental relative rate constants were determined in 50% (v/v) dioxane–water solvent. At 20 °C, dioxane–water solutions of 40% and 60% (v/v) have reported dielectric constants of 43.9 and 26.8, respectively.¹⁷

Regardless of the dielectric constant used in the energy calculations, the correlation is stronger with the values of $\Delta S_{NAC,S}$ calculated by method 1. In method 1, the value of the activation entropy was approximated as $\Delta S_{NAC,S}$, the difference between the entropy of the ground state (which includes all points in the energy landscape) and that of a single conformer (which includes all points in the chosen energy well). The decrease in correlation observed with method 2 indicates that details of well shape (vibrational entropy) make a measurable contribution to the activation entropy. Another factor responsible for the reduced correlation may be the way in which conformations were binned. Three bins of equal size corresponding to *trans*, *gauche*⁺, and *gauche*[−] rotamers were used for rotation about bonds between two *sp*³ centers. The number of rotamers about bonds between *sp*³ and *sp*² hybridized carbons is dependent upon the groups attached to those carbons. To explore this issue, we calculated energy profiles for rotation about the bond between carbonyl and alpha carbons in selected simple carboxylates (Figure 5). Two energy minima are observed in the cases of propionate and 2-methylpropionate. In contrast, six pronounced energy minima are displayed for acetate and for 2,2-dimethylpropionate. The contour plot for 2,2-dimethylbutanoate showing energy as a function of rotation about the bonds between carbonyl and alpha carbons (χ_1) and alpha and beta carbons (χ_2) displays only two minima for rotation about χ_1 for a given value of χ_2 , but the angular values at which these occur are χ_2 dependent. Because the location of the wells for test structures with two minima (at 90° and −90°) were similar to the location of two of the six wells for acetate, and because low probability rotamers corresponding to bins that lack an energy minimum would contribute little to the sum in eq 5, six bins were used for rotation about a bond between *sp*² and *sp*³ centers. Although the majority of the bins defined in this manner contained only a single energy minimum, there were a few cases in which a bin contained multiple closely spaced minima (two or three) and a few cases in which a single minimum was not perfectly centered inside the bin but rather fell close to the bin boundary. The imperfect binning in method 2 may also have contributed to the decreased correlation between the estimated entropy differences and $\ln k_{rel}$ relative to method 1.

Based on the entropies of formation of straight chain alkanes and cycloalkanes (corrected for low frequency motions), Page and Jencks have estimated a loss of 4.5 eu upon freezing an internal rotation and have noted that activation entropies for various cyclization reactions are comparable or smaller.⁶ We estimate a difference in activation entropy between GLUT (four rotatable bonds) and SUCC (three rotatable bonds) of 4.3 eu and a difference between SUCC and 36ETHP (two rotatable bonds) of 5.8 eu in close agreement with the estimate from

(17) Akhadvov, Y. Y. *Dielectric Properties of Binary Solutions*; Pergamon Press: Oxford, 1981.

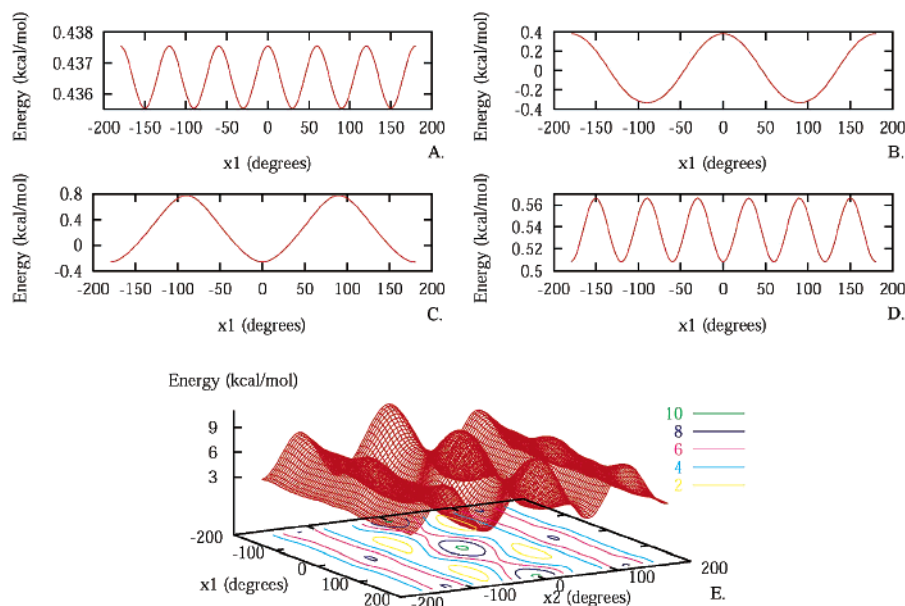


Figure 5. Energy profiles for (A) acetate, (B) propionate, (C) 2-methylpropionate, (D) 2,2-dimethylpropionate, and (E) 2,2-dimethylbutanoate. The grid scan conformational search procedure detailed in the Methods section was performed on each molecule, and minimized energies were calculated using the CHARMM potential function and parameter set. The absolute location of observed minima may be shifted depending on the atoms used in defining the torsions.

experimental data. Differences calculated by method 1 using a dielectric of 80 have a range of 10 eu ($-T\Delta(\Delta S^\ddagger) = 3.0$ kcal/mol) corresponding to a rate enhancement of ~ 160 . This range of reaction rate enhancement is smaller than the range of $\sim 8.0 \times 10^4$ found experimentally between the rates of anhydride formation of GLUT and 36ETHP. The remaining enhancement in reaction rate must therefore be due to enthalpic factors as suggested by Lightstone and Bruice¹. The calculations of Lightstone and Bruice¹ show a difference in enthalpy between the same two extreme compounds, GLUT and 36ETHP, of ~ 4.5 kcal/mol equivalent to a rate enhancement of ~ 2200 times that, which by itself does not explain the rate enhancement observed experimentally. Combining the estimated entropic ($-T\Delta(\Delta S^\ddagger) = 3.0$ kcal/mol) and enthalpic ($\Delta(\Delta H) = 4.5$ kcal/mol) contributions gives a value of $\Delta(\Delta G^\ddagger)$ of 7.5 kcal/mol equivalent to a relative rate enhancement of 35×10^4 very close to the experimentally observed range of rate enhancement (8×10^4).

4. Conclusions

Two methods, one yielding a partial configurational entropy difference and the other a conformational entropy difference, were used to approximate the quantity $\Delta S_{\text{NAC,S}}$, the difference in entropy between all ground state conformers and a single conformer closely resembling the transition state in geometry, for a series of monoesters of dicarboxylic acids undergoing intramolecular condensations to form cyclic anhydrides. When energy calculations were performed using a dielectric constant of 80, both estimates were well correlated with the experimentally determined rate constants relative to the formation of acetic anhydride from *p*-bromophenylacetate and acetate. This result suggests that the reaction rates are correlated with the conformational entropy component of the activation entropy and the contribution arising from a change in librational motions is small. This may explain in part why a previous study that considered mainly entropy differences between single conformations

suggested that the reaction rates correlate exclusively with the enthalpy and not with the entropy of activation.¹ Furthermore, although significantly weaker ($R^2 = 0.73$ and 0.70 by methods 1 and 2, respectively), the correlation holds when calculations are performed using a dielectric of 1 indicating the robustness of the result in light of the fact that the experimental data were obtained in solvent of high dielectric. Although the values of the entropic differences reported here and the enthalpic differences reported previously¹ are well correlated with the logarithm of the relative reaction rates, neither value can by itself account for the total extent of rate enhancement observed experimentally. Not surprisingly, a combination of the calculated enthalpic and entropic effects accounts much better for the observed range of rate enhancements than either of the effects by themselves. The observed increase in rate of intramolecular reactions upon reducing the number of intervening rotatable bonds and/or increasing the size of substituents between reactive moieties has been explained in part by a reduction in volume of the nonproductive region of conformational space.¹⁸ This interpretation is supported by the work presented here. Careful estimates of the contributions of vibrational motions to the entropy of activation show that these contributions are small for all the compounds studied.

Acknowledgment. We gratefully acknowledge the Burroughs Wellcome Fund for supporting this work through its funding of the Johns Hopkins Program in Computational Biology and the NSF for support through Grant MCB-9982945. We thank Drs. J. T. Stivers and J. M. Berg for careful reading of the manuscript and X. Siebert, Dr. J.A. Leyva, and Dr. M. E. Paulaitis for many helpful discussions.

JA0344359

(18) Milstien, S.; Cohen, L. A. *J. Am. Chem. Soc.* **1972**, *94*, 9158.